www.nature.com/cmi

ARTICLE

MEF2C promotes M1 macrophage polarization and Th1 responses

Xibao Zhao[1,5], Qianqian Di[1,5], Han Liu[2,5], Jiazheng Quan[1], Jing Ling[3], Zizhao Zhao[3], Yue Xiao[1], Han Wu[1], Zherui Wu[1], Wengang Song[4], Huazhang An[4]✉ and Weilin Chen[1]✉

The polarization of macrophages to the M1 or M2 phenotype has a pivotal role in inflammation and host defense; however, the underlying molecular mechanism remains unclear. Here, we show that myocyte enhancer factor 2 C (MEF2C) is essential for regulating M1 macrophage polarization in response to infection and inflammation. Global gene expression analysis demonstrated that MEF2C deficiency in macrophages downregulated the expression of M1 phenotypic markers and upregulated the expression of M2 phenotypic markers. MEF2C significantly promoted the expression of interleukin-12 p35 subunit *(Il12a)* and interleukin-12 p40 subunit *(Il12b)*. Myeloid-specific *Mef2c*-knockout mice showed reduced IL-12 production and impaired Th1 responses, which led to susceptibility to *Listeria monocytogenes* infection and protected against DSS-induced IBD in vivo. Mechanistically, we showed that MEF2C directly activated the transcription of *Il12a* and *Il12b*. These findings reveal a new function of MEF2C in macrophage polarization and Th1 responses and identify MEF2C as a potential target for therapeutic intervention in inflammatory and autoimmune diseases.

Keywords: Myocyte enhancer factor 2C; Macrophage polarization; Interleukin-12; T helper type 1 response; Inflammation

Cellular & Molecular Immunology (2022) 19:540–553; https://doi.org/10.1038/s41423-022-00841-w

INTRODUCTION

Macrophages are critical players in immune responses, such as inflammation, immunoregulation and tissue remodeling [1–4]. These cells are essential for the initiation and resolution of pathogen- or damage-induced inflammation [2]. Macrophages are also capable of phagocytosis and antigen presentation, providing these cells with a powerful ability to regulate innate and adaptive immunity and resist pathogen infection [5–7].

Currently, there are at least four definitions of macrophage activation, including terms such as M1 and M2, alternative and classic activation, regulatory macrophages, and subdivisions originating from parent terms [8]. However, the diversity of terminology and inconsistent use of markers to describe macrophage activation might impede research. To avoid confusion, we classified classically activated macrophages (M1) and alternatively activated macrophages (M2) in our research. These populations can be phenotypically polarized by surrounding microenvironmental stimuli to activate specific functional programs [9, 10]. M1 macrophages can be induced by granulocyte-macrophage colony-stimulating factor (GM-CSF) or interferon-γ (IFN-γ) following stimulation with bacterial products such as lipopolysaccharide (LPS), leading to the production of high levels of proinflammatory cytokines, such as interleukin 12 (IL-12) and IL-23, which promote proinflammatory responses. In contrast, M2 macrophages are induced by M-CSF, IL-4, and IL-13. M2 macrophages express high levels of M2-associated phenotypic markers, such as IL-10 and arginase 1 (Arg1), and drive immune regulation and tissue remodeling [11–13]. As a critical feature of the innate immune system, macrophage polarization is a dynamic process that is tightly regulated. Dysregulation of this process can allow bacterial and helminth infection [14, 15], as well as conditions such as inflammation [16], cancer [17, 18], metabolic disorders and insulin resistance [19]. Fibroblast growth factor 2 (FGF2) affects macrophage polarization and is a critical regulator of immunity in the tumor microenvironment [20]. Although macrophage polarization has been intensively studied, the molecular mechanism underlying macrophage polarization remains largely unknown.

IL-12 is a heterodimeric cytokine composed of p35 and p40 subunits (*Il12a and Il12b*), and the p40 subunit is shared by IL-23 [21]. IL-12 plays a crucial role in the regulation of innate and adaptive immune responses during infection and inflammation [22, 23]. Previous studies have demonstrated that IL-12 is a phenotypic marker of M1 macrophages [11, 24]. IL-12-deficient macrophages tend to differentiate into M2 macrophages [25]. IL-12 promotes $CD4^+$ T cell differentiation into T helper 1 (Th1) cells and the production of interferon-γ [21]. Studies have shown that

[1]Guangdong Provincial Key Laboratory of Regional Immunity and Diseases, Department of Immunology, Shenzhen University School of Medicine, Shenzhen 518060, China. [2]Scientific Research Center, Shanghai Public Health Clinical Center, Fudan University, Shanghai 201508, China. [3]Institute of Immunology, Zhejiang University School of Medicine, Hangzhou 310058, China. [4]Shandong Provincial Key Laboratory for Rheumatic Disease and Translational Medicine, The First Affiliated Hospital of Shandong First Medical University & Shandong Provincial Qianfoshan Hospital, Jingshi Road 16766, Jinan, Shandong 250014, China. [5]These authors contributed equally: Xibao Zhao, Qianqian Di, Han Liu. ✉email: anhz@immunol.org; cwl@szu.edu.cn

Received: 18 August 2021 Accepted: 25 January 2022
Published online: 22 February 2022

M1 macrophage polarization can lead to a potent Th1 response and form a link between innate resistance and adaptive immunity [11, 21]. Th1 cells have important immune functions, and abnormal activation can cause inflammation and autoimmune diseases, such as inflammatory bowel disease and collagen-induced arthritis [26, 27].

Myocyte-specific enhancer factor 2c (*Mef2c*) belongs to the MADS-box transcription factor family and contains highly conserved MADS and MEF2 domains in the N-terminus. These domains are essential for DNA binding, dimerization and interactions with other factors [28]. The carboxy-terminal segment is much less conserved and confers transcriptional activation properties [29]. MEF2 is a critical transcriptional switch in the adult body that links metabolism and immunity [30]. Deletion of MEF2A recapitulated PGE2 treatment and abolished type I interferon induction after exposure to innate immune stimuli [31]. Stochastic activation of the hippocampal CREB-pCREB-miR466f-3p-MEF2A axis modulates individual variations in spatial learning and memory capability in inbred mice [32]. MEF2C can activate or enhance gene expression by binding to the promoter region via a consensus A/T-rich DNA sequence known as the MEF2 site [33]. MEF2C is essential for the development and differentiation of bone, neuronal cells, and cardiac and skeletal muscle [34, 35]. In addition, MEF2C also has important functions in myeloid leukemia [36, 37], IFN-I-dependent inflammatory responses [38], and B cell proliferation [39]. Interestingly, MEF2C binding sites were the most highly enriched motifs in a ChIP-seq search for de novo enhancer sequences in *M*. tuberculosis-infected macrophages [40]. This finding indicated that MEF2C plays an important role in macrophage responses to infection and requires further study. Here, we demonstrated that MEF2C promoted M1 macrophage polarization by regulating the expression of macrophage lineage-specific cytokines. Using chromatin immunoprecipitation (ChIP) and double luciferase reporter assays, we revealed that MEF2C was directly involved in the transcriptional regulation of the *Il12a* and *Il12b* subunits. Furthermore, we used myeloid-specific *Mef2c*-knockout ($Mef2c^{flox/flox}$ Lyz2-cre) mice to demonstrate that *Mef2c* deficiency reduced IL-12 production and impaired Th1 responses, leading to susceptibility to *Listeria monocytogenes* infection and resistance to DSS-induced IBD in vivo. These findings reveal a new function of *Mef2c* in macrophage polarization and Th1 responses, suggesting that *Mef2c*-mediated IL-12 transcriptional regulation is crucial for the phenotypic polarization of macrophages and related immune-associated diseases.

MATERIALS AND METHODS

Mice

$Mef2c^{fl/fl}$ mice were purchased from the Jackson Laboratory (Stock No: 025556). Briefly, $Mef2c^{fl/fl}$ mice possess *loxP* sites flanking the second coding exon of the *Mef2c* gene. When crossed with mice that express tissue-specific Cre recombinase, exon 2 of the *Mef2c* gene is deleted in the Cre-expressing tissues of the resulting offspring.

Lyz2-cre mice were purchased from Nanjing Biomedical Research Institute of Nanjing University. $Mef2c^{fl/fl}$ mice were crossed with *Lyz2-cre* mice to obtain $Mef2c^{fl/fl}$ *Lyz2-cre* mice. Murine genotypes were determined by PCR analysis of tail-snip DNA using the following primers: *Mef2c lox* forward: 5′-TTCAGGTGACCTCATTTGAACC-3′; *Mef2c lox* reverse: 5′-GGAGCCATTGCTCATAAGAAAG-3′; *Lyz2-cre* forward: 5′-GAACGCACTGATTTCGACCA-3′; and *Lyz2-cre* reverse: 5′-GCTAACCAGCGTTTTCGTTC-3′.

Mice were maintained and bred in pathogen-free conditions. All animal experiments were performed in accordance with the National Institutes of Health Guide for the Care and Use of Laboratory Animals, and approval was granted by the Institutional Animal Care and Use Committee of Shenzhen University, Shenzhen, China.

Cell culture

M1 and M2 macrophages were obtained from mouse bone marrow cells that were cultured for 5 days in RPMI-1640 medium supplemented with GM-CSF (20 ng/ml, #AF-315-03, Peprotech) or M-CSF (20 ng/ml, # AF-315-02, Peprotech). HEK 293 T and THP1 cells were obtained from the American Type Culture Collection and cultured in DMEM containing 10% fetal bovine serum. All cell cultures were maintained in the appropriate media at 37 °C with 5% CO_2 and 95% humidity.

Plasmids and reagents

Plasmids expressing Flag-tagged full-length *Mef2c* and luciferase reporter plasmids containing wild-type or mutant promoters of *Il12a* and *Il12b* were constructed using standard molecular biology techniques. Antibodies against iNOS (# 13120) and Arg1 (# 93668) were purchased from Cell Signaling Technology. Antibodies against MEF2C (# 10056-1-AP), IFN-γ (# 15365-1-AP), F4/80 (# 28463-1-AP), CD86 (# 13395-1-AP), CD206 (# 18704-1-AP) and β-actin (# 60008) were purchased from Proteintech Group. For flow cytometry, anti-CD11c-APC (# 117309), anti-CD206-PE (# 141705), anti-CD4-FITC (# 100501), anti-IFN-γ-AF647 (# 505816), anti-IL-4-APC (# 504105), anti-CD25-AF700 (# 102024), anti-IL-12-PE/Cy7 (# 505209), anti-F4/80-BV421 (# 123131), anti-CD11b-FITC (# 101206) and 7-AAD (# 420403) were purchased from BioLegend. LPS (# L3024) was purchased from Sigma–Aldrich. Animal-free recombinant murine IL-4 (# AF-214-14) was purchased from Peprotech.

Reactive oxygen species assay

Intracellular ROS levels were measured using a Reactive Oxygen Species Assay Kit (# S0033S, Beyotime Biotechnology) according to the manufacturer's protocol.

Chromatin immunoprecipitation (ChIP) analysis

Chromatin immunoprecipitation assays were performed using EZ-ChIP Chromatin Immunoprecipitation Kits (# 17-371, Millipore) according to the manufacturer's protocol with the following primers: *Il12a* (IP: MEF2C), 5′-ACTGTTAGGGCTAATAGGCAAAC-3′ and 5′-CCTGATGGTTTTACTTTCCTCTG-3′; *Il12b* (IP: MEF2C), 5′-GTTAGCCATTGCCGCCTCTATTC-3′ and 5′-CGTCG AAATCCCAGGTTAAGAG-3′; *Il12a* (IP: PU.1), 5′-GGACTGTGTCTGGTGGCCAA G-3′ and 5′- GAAGCTCATTTAAGGGAGCTGTTCC-3′; *Il12b* (IP: PU.1 and NF-κB), 5′-GATGCACTCAGGGAGGCAAGG-3′ and 5′-CTGACTAGTCTCAATTG CAACACTG-3′; *Il12a* (IP: IRF8), 5′-CCTATCTTCTTCCTGTTTCTACTGCCAC-3′ and 5′-GTGCTGAGGGCTGATTTCAACG-3′; *Il12b* (IP: IRF8), 5′-CCCAGAATG TTTTGACACTAGTTTTCAG-3′ and 5′-GCTCCTGGTGCTTATATACTCTACTCC-3′; and *Il12a* (IP: NF-κB), 5′-CACCCAGTGAGGCTGTCTTGG-3′ and 5′-GAGTT CGAAGCTTGCAATGACAAGC-3′.

Dual-luciferase reporter assays

HEK 293 T cells or Raw 264.7 cells (2×10^4 cells per well) were seeded in 96-well plates and then cotransfected with *Mef2c*-expressing plasmids (100 ng per well), the indicated *Il12a* or *Il12b* luciferase reporter plasmids (80 ng per well) and the Renilla luciferase construct pRL-TK (Promega, for normalization of the transfection efficiency, 10 ng per well). After 24 h, with or without LPS stimulation, the cells were harvested, and dual-luciferase assays were performed using a dual-specific luciferase assay kit (# E1960, Promega) according to the manufacturer's protocols.

Quantitative PCR (qPCR) and ELISA

Total RNA was extracted from cells using RNAiso Plus (#9109, Takara) according to the manufacturer's instructions. Gene expression was determined by Hieff qPCR SYBR Green Master Mix (no ROX) (#11201ES03, Yeasen), and gene expression was normalized to β-actin using the ΔΔCt method. The following gene-specific primers were used: m*Il12a* forward, 5′-CTGTGCCTTGGTAGCATCTA-3′ and reverse, 5′-TTTC ACTCTGTAAGGGTCTG-3′; m*Il12b* forward, 5′- AGGTGCGTTCCTCGTAGAGA-3′ and reverse, 5′-AAAGCCAACCAAGCAGAAGA-3′; m*Il23a* forward, 5′-GCACCTGCTTGACTCTGAC-3′ and reverse, 5′-CGCTGCCACTGCTGACTA-3′; m*Il10* forward, 5′-GCTGCGGACTGCCTTCA-3′ and reverse, 5′-TGCATTAAG GAGTCGGTTAGCA-3′; m*Arg1* forward, 5′-CAGAAGAATGGAAGAGTCAG-3′ and reverse, 5′-CAGATATGCAGGGAGTCACC-3′; m*Chil3* forward, 5′-GGAT GGCTACACTGGAGAAA-3′ and reverse, 5′-AGAAGGGTCACTCAGGATAA-3′; m*Ifng* forward, 5′-GATGCATTCATGAGTATTGCCAAGT-3′ and reverse, 5′-GT GGACCACTCGGATGAGCTC-3′; m*Tbet* forward, 5′-CAACAACCCCTTTGCCA AAG-3′ and reverse, 5′-TCCCCCAAGCAGTTGACAGT-3′; m*Il4* forward, 5′-AGATCACGGCATTTTGAACG-3′ and reverse, 5′-TTTGGCACATCCATCTCCG-3′; m*Gata3* forward, 5′-AGAACCGGCCCCTTATGAA-3′ and reverse, 5′-AGTT CGCGCAGGATGTCC-3′; m*Foxp3* forward, 5′-GGCGAAAGTGGCAGAGAGG TAT-3′ and reverse, 5′-AAGACCCCAGTGGCAGCAGAA-3′; m*Il1b* forward, 5′-A

ACTGTTCCTGAACTCAACTGT-3′ and reverse, 5′-GAGATTTGAAGCTG GATGCTCT-3′; m*Il6* forward, 5′- TAGTCCTTCCTACCCCAATTTCC-3′ and reverse, 5′-TTGGTCCTTAGCCACTCCTTC-3′; m*Tnf* forward, 5′-AAGCCTG TAGCCCACGTCGTA-3′ and reverse, 5′-GGCACCACTAGTTGGTTGTCTTTG-3′; m*Nos2* forward, 5′-CAGCACAGGAAATGTTTCAGC-3′ and reverse, 5′-TAGC CAGCGTACCGGATGA-3′; m*Cox2* forward, 5′-CCCTGAAGCCGTACACATCA-3′ and reverse, 5′-TGTCACTGTAGAGGGCTTTCAATT-3′; m*Mef2c* forward, 5′-AG AAGGCTTATGAGCTGAGCG-3′ and reverse, 5′-ACTCGGTGTACTTGAGCA ACAC-3′; m*Actb* forward, 5′- AGTGTGACGTTGACATCCGT-3′ and reverse, 5′- GCAGCTCAGTAACAGTCCGC-3′; h*IL12B* forward, 5′-TGCCCATTGAGGT CATGGTG-3′ and reverse, 5′- CTTGGGTGGGTCAGGTTTGA-3′; h*IL23A* forward, 5′-CTCAGGGACAACAGTCAGTTC-3′ and reverse, 5′-ACAGGGCTATCAG GGAGCA-3′; h*IL10* forward, 5′-TCAAGGCGCATGTGAACTCC-3′ and reverse, 5′-GATGTCAAACTCACTCATGGCT-3′; h*ARG1* forward, 5′-TGGACAGACTAGGA ATTGGCA-3′ and reverse, 5′-CCAGTCCGTCAACATCAAAACT-3′; and h*ACTB* forward, 5′-TGGAGAAAATCTGGCACCACACC-3′and reverse, 5′-GATGGGCAC AGTGTGGGTGACCC-3′.

ELISA kits (Invitrogen) were used to determine the concentrations of IL-1β (# 88-7013-22), IL-6 (# 88-7064-22), TNF-α (# 88-7346-22), IL-12p70 (# 88-7121-22), and IL-10 (# 88-7105-22) in culture supernatants or serum according to the manufacturer's protocols.

Phagocytosis and bacteria-killing assays

Phagocytosis and bacterial killing were assessed using a gentamicin protection assay. In short, *Listeria monocytogenes*-infected macrophages (MOI = 0.1 or 1) were cultured in medium without antibiotics for 30 min at 37 °C. Subsequently, gentamicin (50 μg/mL) was added, and the cells were incubated for an additional 30 min at 37 °C. Then, the cells were lysed in water for 10 min at 0, 1, 2, 4, and 6 h after the addition of fresh medium without gentamicin. Serial dilutions were plated on BHI plates containing chloramphenicol, and colonies were counted to determine CFUs.

Plasmid transfection and RNA interference assay

Plasmids or siRNA oligos were transfected into cells using jetPRIME (# 114-15, PolyPlus) according to the manufacturer's protocol. At 24 h or 48 h after transfection, the cells were harvested or stimulated with LPS (100 ng/ml) and analyzed by qPCR. The siRNA sequences were as follows: Control siRNA: 5′-UUCUCCGAACGUGUCACGUUU-3′; m*Mef2a* siRNA: 5′-GUGGCAGU-CUUGGAAUGAATT-3′; m*Mef2c* siRNA: 5′-CCCACCUGGCAGCAAGAACAC-3′; m*Mef2d* siRNA: 5′-GAUCCAGCGAAUCACUGAUTT-3′; and h*MEF2C* siRNA: 5′-CACCUGGUAACUUGAACAATT-3′.

RNA sequencing

RNA-seq and data analysis were conducted by Seqhealth Technology Co., Ltd. (Wuhan, China). In brief, total RNA was extracted from LPS-stimulated BMDMs using TRIzol reagent, and DNA was then digested using DNase I. Next, 2 μg of total RNA was used for stranded RNA sequencing library preparation using a KCTM Stranded mRNA Library Prep Kit for Illumina® (Catalog No. DR08402, Wuhan Seqhealth Co., Ltd. China) according to the manufacturer's instructions. PCR products corresponding to 200–500 bps were enriched, quantified and sequenced on a NovaSeq 6000 sequencer (Illumina) with a PE150 model.

Raw sequencing data were first filtered by Trimmomatic (version 0.36). Low-quality reads were discarded, and reads that were contaminated with adaptor sequences were trimmed. Clean data were mapped to the mouse reference genome using STRA software (version 2.5.3a) with default parameters. Differentially expressed genes between groups were identified using the edgeR package (version 3.12.1). A *P* value cutoff of 0.05 and a fold-change cutoff of 1.5 were used to determine the statistical significance of differences in gene expression. Gene ontology (GO) analysis of differentially expressed genes was performed using KOBAS software (version: 2.1.1), and a *P* value cutoff of 0.05 was used to determine statistically significant enrichment.

Listeria monocytogenes infection assay

Listeria monocytogenes bacteria were cultured in BHI broth overnight at 37 °C, centrifuged (5000 × *g* for 5 min at 4 °C) and resuspended in PBS. Age- and sex-matched $Mef2c^{fl/fl}$ and $Mef2c^{fl/fl}$ *Lyz2-cre* mice (aged 8–10 weeks) were intravenously injected with *Listeria monocytogenes* (2×10^5 CFU/mouse). Three days later, serum was collected for ELISA. The mice were euthanized, and the liver and spleen were collected to determine the bacterial load. The livers from *Listeria monocytogenes*-infected mice were fixed and stained with HE and then examined for histological changes under a light microscope. To analyze $CD4^+$ T cell responses, the spleens of *Listeria monocytogenes*-infected mice were isolated, and single-cell suspensions were prepared for qPCR analysis of *Ifng*, *Tbet*, *Il4*, *Gata3* and *Foxp3* expression and flow cytometric analysis of IFN-γ, IL-4 and CD25 expression in CD4 T cells. For cytokine staining, the cells were pretreated with PMA (50 ng/ml, #S7791, Selleck), brefeldin A (3.0 ug/ml, #S7046, Selleck) and ionomycin (1 mg/ml, #SQ23377, MedChemExpress) for 5 h at 37 °C before flow cytometric analysis.

Induction of experimental colitis

Age- and sex-matched groups of littermates (aged 8–10 weeks) were administered 3% (w/v) DSS (#160110, MP Biomedical) in drinking water for 7 days, followed by a 2-day recovery period with normal drinking water before sacrifice. The colons were cut into small pieces in 500 μl of PBS and then centrifuged at 400 × *g* for 5 min. The supernatants were used to analyze IL-1β, IL-6, TNF-α and IL-12p70 production in colon tissue by ELISA, and the cell pellets were used for qPCR analysis of *Il1b*, *Il6*, *Tnf*, *Il12a*, *Il12b* and *Cox2* mRNA expression in the colon tissue from $Mef2c^{flox/flox}$ and $Mef2c^{flox/flox}$ *Lyz2-cre* mice.

Isolation of colonic lamina propria mononuclear cells (LPMCs)

Experimental colitis was induced in $Mef2c^{flox/flox}$ and $Mef2c^{flox/flox}$ *Lyz2-cre* mice with DSS. Freshly isolated colon tissues were opened longitudinally and washed with sterile HBSS. The colons were cut into small pieces (<5 mm) and washed three times with HBSS. The tissues were then incubated in HBSS (with 5 mM EDTA and 1 mM DTT, but without Ca^{2+} and Mg^{2+}) for 20 min at 37 °C in a 200 rpm shaking incubator. After the suspended cells were removed, the colon pieces were collected in 50 ml tubes containing warmed digestion solution (containing 0.5 mg/ml DNase I and 0.5 mg/ml collagenase D in PBS). All colon pieces were incubated in digestion solution for 45 min at 37 °C in a 200 rpm shaking incubator. A Percoll gradient was used to isolate LPMCs from cell suspensions after adequate digestion. IFN-γ, IL-4 and CD25 expression in $CD4^+$ T cells and CD11c, CD206 and IL-12 expression in macrophages were analyzed by flow cytometry. For cytokine staining, the cells were pretreated with PMA (50 ng/ml, #S7791, Selleck), brefeldin A (3.0 ug/ml, #S7046, Selleck) and ionomycin (1 mg/ml, #SQ23377, MedChemExpress) for 5 h at 37 °C before flow cytometric analysis.

Statistical analyses

The data are presented as the means ± SD of one of three independent experiments, and the data were analyzed by GraphPad Prism. To analyze the differences between two groups, a two-tailed Student's *t* test was used. Mouse survival was analyzed using the Kaplan–Meier method. $P < 0.05$ was considered to indicate statistical significance.

RESULTS

Mef2c is involved in macrophage polarization

Macrophages are a heterogeneous population of immune cells that change their phenotype and physiology in response to cytokines and microbial signals. M1 macrophages and M2 macrophages have different patterns of cytokine expression. M1 macrophages are engaged in inflammatory, microbicidal and tumoricidal activities and are characterized as having an $IL\text{-}12^{high}IL\text{-}10^{low}$ phenotype, whereas M2 macrophages are involved in the resolution of inflammation. To investigate whether *Mef2c* is involved in macrophage polarization, we crossed $Mef2c^{flox/flox}$ mice, which possess *loxP* sites flanking the second coding exon of the *Mef2c* gene (Fig. S1a), with *Lyz2-cre* mice to obtain $Mef2c^{flox/flox}$ *Lyz2-cre* mice in which *Mef2c* is ablated (Fig. S1b and c). Global gene expression analysis indicated that *Mef2c* deficiency affected the expression of a large number of genes (Fig. S2a). Among these differentially expressed genes (DEGs), M1 macrophage markers, such as *Il12b*, *Nos2* and *Il12a*, were downregulated, whereas the expression of the M2 macrophage markers *Arg1* and *Chil3* was upregulated (Fig. 1a and b). Gene ontology (GO) analysis indicated that *Mef2c* positively regulated IL-12 production (Fig. S2b).

To further investigate the involvement of *Mef2c* in macrophage polarization, we used GM-CSF and M-CSF to induce M1 and M2

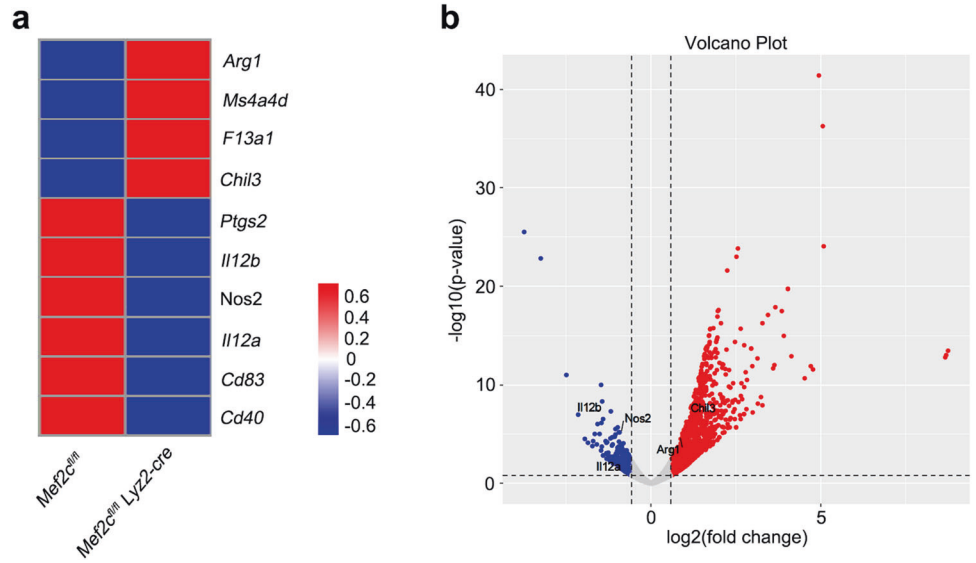

Fig. 1 *Mef2c* is involved in macrophage polarization. **a** *Mef2c*$^{flox/flox}$ and *Mef2c*$^{flox/flox}$ *Lyz2-cre* macrophages were stimulated with LPS (100 ng/ml) for 2 h. Total RNA was extracted, and RNA-seq analysis was performed. Heatmaps of the selected gene panels are shown. **b** Volcano plot of the differentially expressed genes (downregulated and upregulated genes are shown in blue and red, respectively)

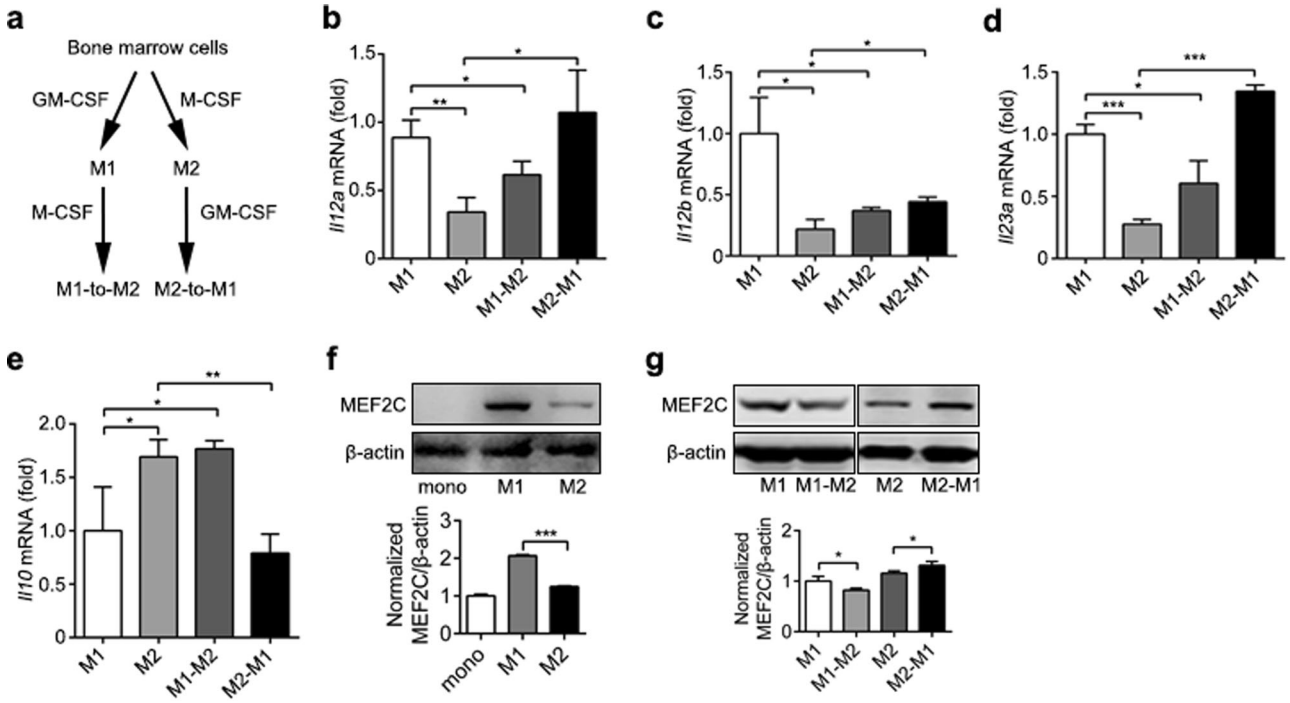

Fig. 2 High expression of MEF2C in M1 macrophages. **a** Schematic diagram of the strategy used to induce M1 or M2 and M1-to-M2 or M2-to-M1 polarization. Bone marrow-derived cells were differentiated for 5 days into M1 macrophages with GM-CSF (20 ng/ml) and into M2 macrophages with M-CSF (20 ng/ml). On Day 5, GM-CSF-induced M1 macrophages were induced with M-CSF (20 ng/ml)-containing medium for 24 h to undergo M1-to-M2 polarization, and on Day 5, M-CSF-induced M2 macrophages were induced with GM-CSF (20 ng/ml)-containing medium for 24 h to undergo M2-to-M1 polarization. **b**–**e** qPCR analysis of *Il12a* (b), *Il12b* (c), *Il23a* (d) and *Il10* (e) expression in macrophages following M1, M2, M1-to-M2 or M2-to-M1 polarization. **f** Immunoblot analysis of MEF2C expression in monocytes collected on Day 0 (mono) or macrophages following M1 or M2 polarization. **g** Immunoblot analysis of MEF2C expression in macrophages following M1-to-M2 or M2-to-M1 polarization. The data are representative of three independent experiments. The data represent the mean ± SD. **P* < 0.05, ***P* < 0.01, ****P* < 0.001

macrophage differentiation, respectively. We also cultured M1 macrophages with M-CSF to induce M1-to-M2 polarization and M2 macrophages with GM-CSF to induce M2-to-M1 polarization (Fig. 2a). We then used qPCR to analyze the mRNA expression of *Il12a*, *Il12b*, *Il23a*, and *Il10* in the cells. The changes in the expression of the cytokines demonstrated that the culture conditions successfully induced macrophage phenotypic polarization with plasticity (Fig. 2b–e). To explore the possible function of *Mef2c* in the inflammatory process and macrophage polarization, we analyzed the level of MEF2C protein in M1 and M2 macrophages. Immunoblotting showed that MEF2C protein levels were higher in bone marrow-derived macrophages (BMDMs)

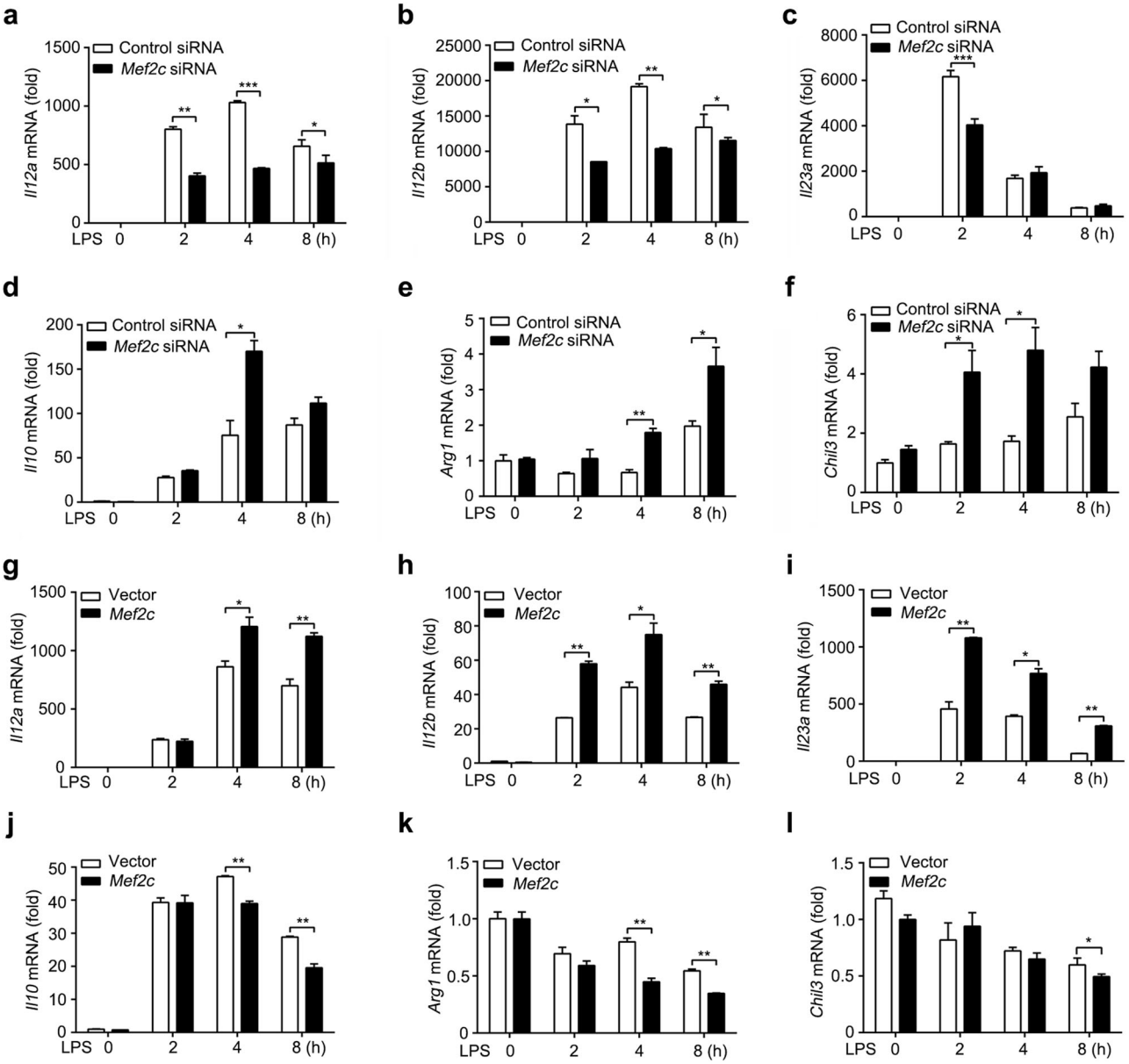

Fig. 3 *Mef2c* influences the expression of macrophage polarization-specific genes. **a**–**f** Bone marrow-derived cells were differentiated for 5 days into M1 macrophages by stimulation with GM-CSF (20 ng/ml). M1 macrophages were then transfected with control or *Mef2c* siRNA for 48 h and then stimulated with LPS (100 ng/ml) for the indicated times. qPCR analysis of *Il12a* (**a**), *Il12b* (**b**), *Il23a* (**c**), *Il10* (**d**), *Arg1* (**e**), and *Chil3* (**f**) mRNA expression. **g**–**l** Bone marrow-derived cells were differentiated for 5 days into M2 macrophages by stimulation with M-CSF (20 ng/ml). M2 macrophages were transfected with vector or *Mef2c* expression plasmid for 48 h and then stimulated with LPS (100 ng/ml) for the indicated times. qPCR analysis of *Il12a* (**g**), *Il12b* (**h**), *Il23a* (**i**), *Il10* (**j**), *Arg1* (**k**), and *Chil3* (**l**) mRNA expression. The data are representative of three independent experiments. The data represent the mean ± SD. $^{*}P < 0.05$, $^{**}P < 0.01$, $^{***}P < 0.001$

differentiated with GM-CSF (M1) than in those differentiated with M-CSF (M2) (Fig. 2f). Treating M1 macrophages with M-CSF resulted in relatively lower levels of MEF2C protein in the converted M2 macrophages (M1-to-M2), whereas treating M2 macrophages with GM-CSF resulted in relatively higher levels of MEF2C protein in the converted M1 macrophages (M2-to-M1) (Fig. 2g). Collectively, these data suggest that *Mef2c* is involved in macrophage polarization.

Mef2c influences the expression of macrophage polarization lineage-specific genes

We next investigated the ability of *Mef2c* to regulate the expression of M1 and M2 macrophage phenotypic markers. Since our results showed that MEF2C protein levels were higher in M1 macrophages than in M2 macrophages, we analyzed the effects of knocking down *Mef2c* in M1 macrophages and overexpressing *Mef2c* in M2 macrophages. qPCR analysis showed that *Mef2c* knockdown in M1 macrophages inhibited LPS-induced expression of the M1 phenotypic markers *Il12a* (Fig. 3a), *Il12b* (Fig. 3b) and *Il23a* (Fig. 3c) but increased LPS-induced expression of the M2 macrophage phenotypic markers *Il10* (Fig. 3d), *Arg1* (Fig. 3e) and *Chil3* (Fig. 3f). To further confirm these results, we knocked down *MEF2C* in THP1 cells and verified that the specific siRNA could efficiently inhibit *MEF2C* expression (Fig. S3a). The results showed that *MEF2C* knockdown decreased *IL12B* (Fig. S3b) and *IL23A* (Fig. S3c) expression but increased *IL10* (Fig. S3d) and *ARG1* (Fig. S3e) expression in LPS-stimulated THP1 cells. In addition, we found that *Mef2c* did not affect NF-κB or MAPK pathway activation in macrophages (Fig. S3f).

In addition, our results demonstrated that *Mef2c* overexpression in M2 macrophages increased the expression of the M1 macrophage phenotypic markers *Il12a* (Fig. 3g), *Il12b* (Fig. 3h) and *Il23a* (Fig. 3i) but decreased the expression of the M2 macrophage phenotypic markers *Il10* (Fig. 3j), *Arg1* (Fig. 3k) and *Chil3* (Fig. 3l). *Mef2a* and *Mef2d* also belong to the MADS-box transcription factor family, and we next investigated whether *Mef2a* and *Mef2d* could regulate *Il12a*, *Il12b* and *Il10* expression. We first designed *Mef2a*- and *Mef2d*-specific siRNAs and found that these siRNAs efficiently inhibited *Mef2a* (Fig. S4a) and *Mef2d* (Fig. S4e) expression in macrophages. The qPCR results showed that *Mef2a* knockdown increased *Il12a* (Fig. S4b), *Il12b* (Fig. S4c) and *Il10* (Fig. S4d) expression in macrophages. Moreover, *Mef2d* knockdown promoted LPS-induced *Il12a* (Fig. S4f), *Il12b* (Fig. S4g) and *Il10* (Fig. S4h) expression in macrophages. These results suggested that *Mef2c* plays a different role in regulating inflammatory gene expression than *Mef2a* or *Mef2d*. Taken together, these results indicate that *Mef2c* affects the expression of macrophage polarization lineage-specific genes by promoting the expression of M1 macrophage markers and inhibiting the expression of M2 macrophage markers.

Mef2c deficiency impairs M1 macrophage polarization

We next used myeloid-specific *Mef2c* knockout ($Mef2c^{flox/flox}$ *Lyz2-cre*) mice to further investigate the role of *Mef2c* in macrophage polarization in vitro and in vivo. In accordance with the knockdown experiments, qPCR analysis showed that *Mef2c* deficiency suppressed the expression of the LPS-induced M1 macrophage markers *Il12a* (Fig. 4a), *Il12b* (Fig. 4b) and *Il23a* (Fig. 4c) and promoted the expression of the LPS-induced M2 macrophage markers *Il10* (Fig. 4d), *Arg1* (Fig. 4e) and *Chil3* (Fig. 4f). Immunoblot analysis also indicated that *Mef2c* knockout decreased LPS-induced iNOS expression (Fig. 4g) and increased IL-4-induced ARG1 expression (Fig. 4h). We monitored macrophage phenotype by flow cytometric analysis of CD11c and CD206 as phenotypic markers of M1 and M2 macrophages, respectively. We found that CD11c expression was downregulated in *Mef2c*-deficient macrophages, whereas CD206 was upregulated (Fig. 4i), suggesting that *Mef2c* deficiency impairs M1 macrophage polarization.

Subsequently, we investigated the effects of *Mef2c* deficiency on macrophage polarization in vivo. $Mef2c^{flox/flox}$ and $Mef2c^{flox/flox}$ *Lyz2-cre* mice received an intraperitoneal injection of LPS, and peritoneal macrophages were collected 2 h later. qPCR analysis showed that *Mef2c* deficiency suppressed the expression of the M1 macrophage markers *Il12a* and *Il12b* in vivo but promoted the expression of the M2 macrophage markers *Il10* and *Arg1* (Fig. 4j). Previous studies have shown that IL-10 signaling is important for inflammatory gene expression [41]. To exclude the effect of IL-10 overproduction on inflammatory gene expression in *Mef2c*-deficient mice/macrophages, we used an IL-10R antibody to block IL-10 signaling. The results showed that blocking IL-10 signaling could significantly promote the expression of the inflammatory genes *Il12a*, *Il12b* and *Il23a* in $Mef2c^{flox/flox}$ and $Mef2c^{flox/flox}$ *Lyz2-cre* macrophages both in vitro (Fig. S5a) and in vivo (Fig. S5b). However, $Mef2c^{flox/flox}$ macrophages still expressed higher levels of the LPS-induced inflammatory genes *Il12a*, *Il12b* and *Il23a* than $Mef2c^{flox/flox}$ *Lyz2-cre* macrophages both in vitro (new Fig. S5a) and in vivo (new Fig. S5b), indicating that *Mef2c* regulated inflammatory gene expression independent of IL-10 signaling. These results suggest that *Mef2c* deficiency impairs M1 macrophage polarization both in vitro and in vivo.

Mef2c-deficient mice show increased susceptibility to *Listeria monocytogenes* infection

Polarization influences the phenotype and function of macrophages. To investigate the effect of *Mef2c* deficiency on the antibacterial innate immune response in vivo, we challenged $Mef2c^{flox/flox}$ and $Mef2c^{flox/flox}$ *Lyz2-cre* mice with *Listeria monocytogenes*. The ELISA results indicated that IL-12 levels in the serum of $Mef2c^{flox/flox}$ *Lyz2-cre* mice were significantly lower than those of $Mef2c^{flox/flox}$ mice (Fig. 5a). We also observed that the levels of the inflammatory cytokines IL-6 (Fig. 5b) and TNF-α (Fig. 5c) in the serum of $Mef2c^{flox/flox}$ *Lyz2-cre* mice were lower than those of $Mef2c^{flox/flox}$ mice. In contrast, IL-10 levels in the serum of $Mef2c^{flox/flox}$ *Lyz2-cre* mice were higher than those of $Mef2c^{flox/flox}$ mice (Fig. 5d). These results revealed that the inflammatory response to *Listeria monocytogenes* infection was impaired in *Mef2c*-deficient mice. To evaluate the ability of *Mef2c* to regulate *Listeria monocytogenes* clearance in vivo, we determined the bacterial burden in the spleen and liver in $Mef2c^{flox/flox}$ and $Mef2c^{flox/flox}$ *Lyz2-cre* mice after *Listeria monocytogenes* infection. The colony formation assays showed that the bacterial burden in the spleen and liver was significantly increased in *Mef2c*-deficient mice, indicating that *Mef2c*-deficient mice had a lower ability to resist *Listeria monocytogenes* infection than wild-type control mice (Figs. 5e and f). However, a significant difference in the bacterial burden in the livers of $Mef2c^{flox/flox}$ and $Mef2c^{flox/flox}$ *Lyz2-cre* mice was observed only on Day 5 after *Listeria monocytogenes* infection, suggesting that *Mef2c* affects adaptive immunity by regulating macrophage polarization and cytokine production. In addition, we observed that the pathological abscesses induced in the spleen and liver by *Listeria monocytogenes* infection were more serious in $Mef2c^{flox/flox}$ *Lyz2-cre mice* than in $Mef2c^{flox/flox}$ mice (Fig. 5g). The formation of microabscesses is a histological hallmark of *Listeria monocytogenes*-infected livers. Hematoxylin and eosin (HE) staining revealed more microabscesses in $Mef2c^{flox/flox}$ *Lyz2-cre mice* than in $Mef2c^{flox/flox}$ mice (Fig. 5h). More importantly, $Mef2c^{flox/flox}$ *Lyz2-cre* mice showed lower resistance to *Listeria monocytogenes* infection in terms of overall survival than $Mef2c^{flox/flox}$ mice (Fig. 5i). These results suggest that *Mef2c* deficiency increases the susceptibility of $Mef2c^{flox/flox}$ *Lyz2-cre* mice to *Listeria monocytogenes* infection.

To further explore the mechanism of *Mef2c* in the host response against *Listeria monocytogenes* infection, we evaluated *Listeria monocytogenes* killing ability and ROS production in macrophages. *Mef2c* deficiency damaged the capacity of macrophages to kill bacteria but did not affect the engulfment of *Listeria monocytogenes* (Fig. 5j and Fig. S6a). Furthermore, we observed that *Mef2c*-deficient macrophages produced less ROS than their wild-type counterparts (Fig. 5k). M1 macrophage polarization promoted the acquisition of antigen-presenting functions and IL-12 production, leading to efficient induction of Th1 responses. The qPCR results showed that splenocytes from *Listeria monocytogenes*-infected $Mef2c^{flox/flox}$ *Lyz2-cre mice* expressed less *Ifng* and *Tbet* mRNA, which are markers of a Th1 response, than those from $Mef2c^{flox/flox}$ mice (Fig. 5l), whereas there was no difference in the mRNA expression levels of the Th2 markers *Il4* and *Gata3* (Fig. S6b) or the Treg marker *Foxp3* (Fig. S6c). We also used flow cytometry to analyze $CD4^+$ T cell differentiation in mice after *Listeria monocytogenes* infection. The frequency of $CD4^+$ IFN-γ^+ T cells among the splenocytes of $Mef2c^{flox/flox}$ *Lyz2-cre* mice was significantly lower than that among the splenocytes of $Mef2c^{flox/flox}$ mice, indicating an impaired Th1 response against *Listeria monocytogenes* infection in $Mef2c^{flox/flox}$ *Lyz2-cre* mice (Fig. 5m). However, *Mef2c* deficiency in macrophages had no effect on Th2 (Fig. S6d) or Treg (Fig. S6e) differentiation. We also evaluated the potential of culture supernatants derived from wild-type or *Mef2c*-deficient macrophages to affect the differentiation of T cells in vitro. Flow cytometric analysis revealed a higher frequency of $CD4^+$ IFN-γ^+ T cells in the presence of wild-type macrophage culture supernatant than in the presence of *Mef2c*-deficient macrophage culture supernatant (Fig. 5n). These results demonstrate that *Mef2c* deficiency increases susceptibility to *Listeria monocytogenes* infection by suppressing M1 macrophage polarization and subsequently initiating Th1 adaptive immune responses.

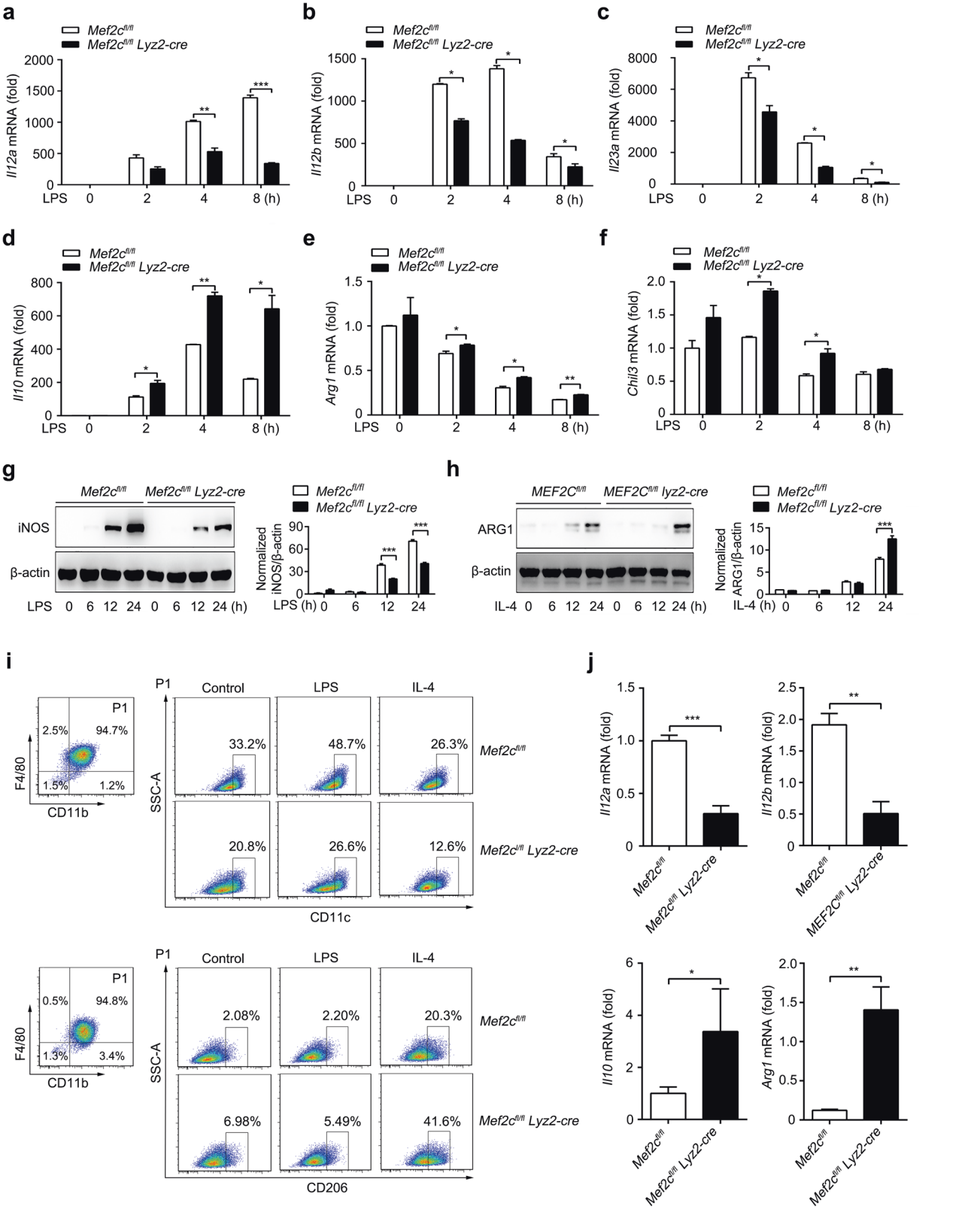

Fig. 4 *Mef2c* deficiency impairs macrophage polarization. qPCR analysis of *Il12a* (**a**), *Il12b* (**b**), *Il23a* (**c**), *Il10* (**d**), *Arg1* (**e**), and *Chil3* (**f**) mRNA expression in $Mef2c^{flox/flox}$ and $Mef2c^{flox/flox}$ *Lyz2-cre* peritoneal macrophages stimulated with LPS (100 ng/ml) for the indicated times. **g** Immunoblot analysis of iNOS expression in $Mef2c^{flox/flox}$ and $Mef2c^{flox/flox}$ *Lyz2-cre* peritoneal macrophages stimulated with LPS (100 ng/ml) for the indicated times. **h** Immunoblot analysis of ARG1 expression in $Mef2c^{flox/flox}$ and $Mef2c^{flox/flox}$ *Lyz2-cre* peritoneal macrophages stimulated with IL-4 (10 ng/ml) for the indicated times. **i** Flow cytometric analysis of CD11c and CD206 expression by $Mef2c^{flox/flox}$ and $Mef2c^{flox/flox}$ *Lyz2-cre* peritoneal macrophages stimulated with LPS (100 ng/ml) or IL-4 (10 ng/ml) for 16 h. **j** qPCR analysis of *Il12a*, *Il12b*, *Il10*, and *Arg1* mRNA expression by peritoneal macrophages collected from $Mef2c^{flox/flox}$ and $Mef2c^{flox/flox}$ *Lyz2-cre* mice 2 h after intraperitoneal injection of LPS (5 mg/kg). The data are representative of three independent experiments. The data represent the mean ± SD. $^{*}P < 0.05$, $^{**}P < 0.01$, $^{***}P < 0.001$

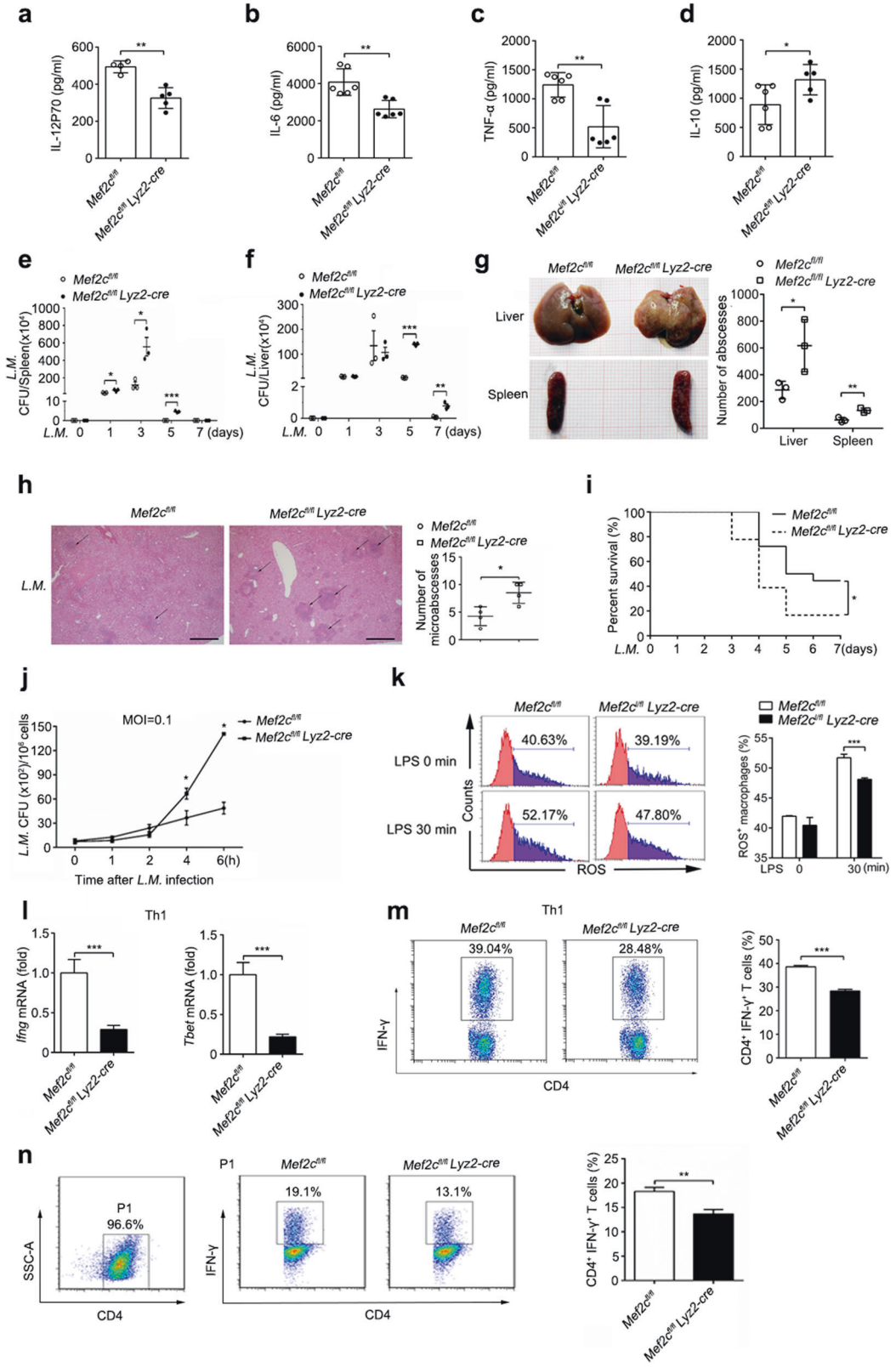

Mef2c deficiency attenuates experimental murine colitis in vivo

Inflammatory bowel disease is closely related to the abnormal activation of macrophages and Th1 cells. We further investigated the effects of *Mef2c* deficiency on DSS-induced acute colitis in mice. As shown in Fig. 6a, colitis-induced body weight loss was significantly alleviated in *Mef2c*$^{flox/flox}$ *Lyz2-cre* mice compared with *Mef2c*$^{flox/flox}$ mice. Furthermore, the disease activity index (diarrhea and rectal bleeding) was obviously reduced in *Mef2c*$^{flox/flox}$ *Lyz2-cre* mice compared with *Mef2c*$^{flox/flox}$ mice (Fig. 6b). Similarly, colon

Fig. 5 *Mef2c* deficiency reduces the host response to Listeria monocytogenes infection. ELISA analysis of IL-12p70 (**a**), IL-6 (**b**), TNF-α (**c**), and IL-10 (**d**) concentrations in the serum of $Mef2c^{flox/flox}$ and $Mef2c^{flox/flox}$ *Lyz2-cre* mice 3 days after intravenous injection of *Listeria monocytogenes* (2×10^5 CFU/mouse). *Listeria monocytogenes* burdens in the spleens (**e**) and livers (**f**) of $Mef2c^{flox/flox}$ and $Mef2c^{flox/flox}$ *Lyz2-cre* mice on Days 0, 1, 3 5, and 7 after intravenous injection of *Listeria monocytogenes* (2×10^5 CFU/mouse). Liver abscesses in $Mef2c^{flox/flox}$ and $Mef2c^{flox/flox}$ *Lyz2-cre* mice were evaluated 3 days after intravenous injection of *Listeria monocytogenes* (2×10^5 CFU/mouse) by light microscopy (**g**) and HE staining (**h**); scale bar = 200 μm. **i** Survival of $Mef2c^{flox/flox}$ and $Mef2c^{flox/flox}$ *Lyz2-cre* mice administered *Listeria monocytogenes* (5×10^5 CFU/mouse) by intravenous injection ($n = 20$ per group). **j** Pathogen burden in peritoneal macrophages isolated from $Mef2c^{flox/flox}$ and $Mef2c^{flox/flox}$ *Lyz2-cre* mice infected with *Listeria monocytogenes* (MOI = 0.1) for the indicated times. **k** Flow cytometric analysis of ROS production by peritoneal macrophages isolated from $Mef2c^{flox/flox}$ and $Mef2c^{flox/flox}$ *Lyz2-cre* mice and stimulated with LPS (100 ng/ml) for the indicated times. **l** qPCR analysis of *Ifng* and *Tbet* expression in spleen cells obtained from $Mef2c^{flox/flox}$ and $Mef2c^{flox/flox}$ *Lyz2-cre* mice 3 days after intravenous injection of *Listeria monocytogenes* (2×10^5 CFU/mouse) and cultured for 48 h with gentamicin in the presence of anti-CD3 and anti-CD28 antibodies. **m** Flow cytometric analysis of IFN-γ expression in $CD4^+$ T cells obtained from the spleens of $Mef2c^{flox/flox}$ and $Mef2c^{flox/flox}$ *Lyz2-cre* mice 3 days after intravenous injection of *Listeria monocytogenes* (2×10^5 CFU/mouse). **n** Naïve $CD4^+$ T cells were sorted from lymph nodes obtained from wild-type mice and cultured in the presence of anti-CD3, anti-CD28, and anti-IL-4 antibodies and supernatant from LPS-stimulated wild-type or *Mef2c*-deficient macrophages prior to the induction of Th1 cell differentiation in vitro. The proportion of $CD4^+$ IFN-γ^+ T cells was then analyzed by flow cytometry. The data are representative of three independent experiments. The data represent the mean ± SD. $^*P < 0.05$, $^{**}P < 0.01$, $^{***}P < 0.001$

length was significantly increased in $Mef2c^{flox/flox}$ *Lyz2-cre* mice compared with $Mef2c^{flox/flox}$ mice (Fig. 6c). Less inflammatory cell infiltration and only slight epithelial damage were observed in the colons of $Mef2c^{flox/flox}$ *Lyz2-cre* mice after colitis induction than in those of $Mef2c^{flox/flox}$ mice (Fig. 6d). qPCR analysis showed lower levels of proinflammatory cytokines and mediators (such as *Il1b*, *Il6*, *Tnf*, *Nos2*, *Il12a*, *Il12b*, and *Cox2*) in the colons of $Mef2c^{flox/flox}$ *Lyz2-cre* mice after colitis induction than in the colons of control $Mef2c^{flox/flox}$ mice (Fig. 6e). ELISA also showed significantly lower levels of IL-1β, IL-6, TNF-α, and IL-12 production in the colons of $Mef2c^{flox/flox}$ *Lyz2-cre* mice after colitis induction than in the colons of $Mef2c^{flox/flox}$ mice (Fig. 6f). These results indicated that *Mef2c* deficiency attenuated DSS-induced acute colitis in mice in vivo.

Immunofluorescence analysis showed that compared with that in $Mef2c^{flox/flox}$ mice, CD86 expression was decreased in $F4/80^+$ macrophages in colon tissue of $Mef2c^{flox/flox}$ *Lyz2-cre* mice (Fig. 7a), while CD206 expression was increased (Fig. 7b), suggesting that *Mef2c* deficiency inhibited macrophage M1 polarization during DSS-induced colitis. We used flow cytometry to analyze macrophage polarization by measuring the expression of CD11c and CD206 as phenotypic markers of M1 and M2 macrophages, respectively. The results showed that CD11c expression was downregulated in the colons of $Mef2c^{flox/flox}$ *Lyz2-cre* mice after colitis induction compared with that in the colons of $Mef2c^{flox/flox}$ mice (Fig. 7c), while CD206 expression was upregulated (Fig. 7d). Furthermore, flow cytometric analysis showed fewer $IL\text{-}12^+$ macrophages in the colons of $Mef2c^{flox/flox}$ *Lyz2-cre* mice after colitis induction than in the colons of $Mef2c^{flox/flox}$ mice (Fig. 7e). We also used flow cytometry to analyze IFN-γ production by $CD4^+$ T cells in the colon tissues of mice. The frequency of $CD4^+$ IFN-γ^+ T cells in the colon tissues of $Mef2c^{flox/flox}$ *Lyz2-cre* mice was significantly lower than that in the colons of $Mef2c^{flox/flox}$ mice, indicating an impaired Th1 response in $Mef2c^{flox/flox}$ *Lyz2-cre* mice in vivo (Fig. 7f). These results were confirmed by immunohistochemical analysis showing significantly reduced levels of IFN-γ expression in the colons of $Mef2c^{flox/flox}$ *Lyz2-cre* mice after colitis induction (Fig. 7g), thus providing further evidence that *Mef2c* deficiency impairs the Th1 response in the colons of $Mef2c^{flox/flox}$ *Lyz2-cre* mice. However, conditional *Mef2c* deficiency had no effect on Th2 (Fig. S7a) or Treg (Fig. S7b) differentiation. These data indicate that *Mef2c* deficiency suppresses the generation of proinflammatory macrophages and impairs Th1 responses in mice with experimental colitis.

MEF2C directly regulates the transcription of *Il12a* and *Il12b*

To investigate the molecular mechanism by which *Mef2c* regulates macrophage polarization, we performed double luciferase reporter gene assays on macrophages transfected with the *Il12a* and *Il12b* promoter luciferase reporter plasmids. *Mef2c* upregulated the luciferase reporter activity of the *Il12a* (Fig. 8a) and *Il12b* (Fig. 8b) promoters. These results were confirmed in ChIP assays showing that MEF2C binds directly to the promoters of *Il12a* and *Il12b* (Fig. 8c, d). We then used the JASPAR database (http://jaspar.genereg.net/) to predict MEF2C binding sites and constructed mutant *Il12a* and *Il12b* promoter luciferase reporter plasmids by deleting the predicted MEF2C binding sites. Double luciferase reporter gene assays showed that the expression of the mutant forms of the *Il12a* (Fig. 8e) and *Il12b* (Fig. 8f) promoters was not regulated by *Mef2c*. Since the binding of MEF2C to the *Il12a* and *Il12b* promoters is dynamic, to further investigate the mechanism of the direct regulation of *Il12a* and *Il12b* expression by *Mef2c* after LPS exposure, we transfected wild-type and mutant *Il12a* or *Il12b* promoter luciferase reporter plasmids into Raw 264.7 cells and then stimulated the cells with LPS. The results revealed that *Mef2c* could increase wild-type *Il12a* or *Il12b* but not mutant *Il12a* or *Il12b* luciferase reporter gene expression after LPS stimulation (Fig. 8g and h). To confirm these results, we transfected wild-type and mutant *Il12a* or *Il12b* luciferase reporter plasmids into HEK 293 T cells with or without the *Myd88* plasmid and obtained similar results (Fig. S8a and b). These data verified that *Mef2c* could directly regulate *Il12a* and *Il12b* expression after LPS exposure. Studies have shown that many transcription factors can regulate IL-12 production, such as PU.1, IRF8 and NK-κB [42–44]. Next, we investigated whether *Mef2c* deficiency affected the binding of other transcription factors to the *Il12a* and *Il12b* promoters. The ChIP assay showed that *Mef2c* deficiency suppressed PU.1 binding to the *Il12a* (Fig. S8c) and *Il12b* (Fig. S8d) promoters and induced IRF8 binding to the *Il12a* (Fig. S8e) and *Il12b* (Fig. S8f) promoters but had no effect on NF-κB (Fig. S8g and h). The results suggested that *Il12a* and *Il12b* expression might be involved in the regulation of multiple transcription factors. Taken together, these results indicate that MEF2C affects macrophage polarization through direct transcriptional regulation of *Il12a* and *Il12b*.

DISCUSSION

In the present study, we uncovered a previously unappreciated role for the transcription factor *Mef2c*, which is involved in promoting M1 macrophage polarization and regulating the Th1 response. These results suggest that *Mef2c* plays an important role in innate and adaptive immunity. Macrophage plasticity allows for efficient changes in phenotype and physiology in response to cytokines and microbial signals [45]. M-CSF and GM-CSF are involved in the regulation of macrophage heterogeneity. Based on differences in phenotype and function, macrophages can be divided into M1 (classically activated) or M2 (alternatively activated) phenotypes [6]. Immunoblot analysis revealed that M1 macrophages expressed higher levels of *Mef2c* protein than M2

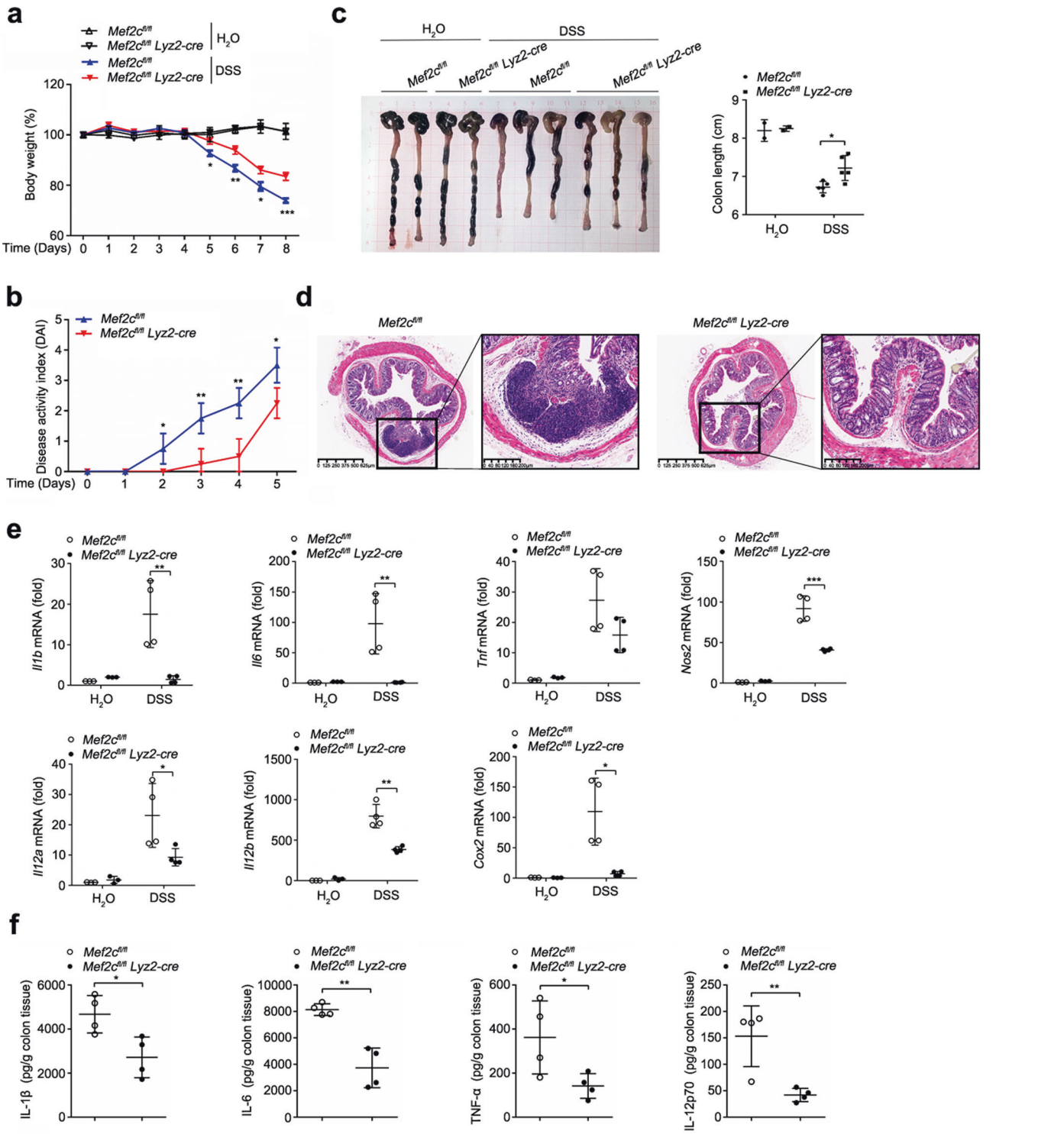

Fig. 6 *Mef2c*$^{flox/flox}$ *Lyz2-cre* mice show attenuated experimental colitis in vivo. *Mef2c*$^{flox/flox}$ and *Mef2c*$^{flox/flox}$ *Lyz2-cre* mice were administered drinking water with or without 3% DSS for 7 days to induce acute colitis, followed by a 2-day recovery period with normal drinking water. Body weight changes (**a**) and DAI scores (**b**) in DSS-induced experimental colitis mice. **c** Gross morphology of colons from *Mef2c*$^{flox/flox}$ and *Mef2c*$^{flox/flox}$ *Lyz2-cre* mice and colon lengths. **d** HE-stained images of colon sections. **e** qPCR analysis of *Il1b*, *Il6*, *Tnf*, *Il12a*, *Il12b*, and *Cox2* mRNA expression in the colons of *Mef2c*$^{flox/flox}$ and *Mef2c*$^{flox/flox}$ *Lyz2-cre* mice. **f** ELISA analysis of IL-1β, IL-6, TNF-α, and IL-12p70 production in the colons of *Mef2c*$^{flox/flox}$ and *Mef2c*$^{flox/flox}$ *Lyz2-cre* mice. The data are representative of three independent experiments. The data represent the mean ± SD. **P* < 0.05, ***P* < 0.01, ****P* < 0.001

macrophages. Moreover, we demonstrated the plasticity of *Mef2c* expression in macrophages during the conversion of the M1 and M2 phenotypes. These findings suggest that *Mef2c* plays an important role in regulating macrophage polarization.

M1 and M2 macrophages differ in their patterns of cytokine expression. M1 macrophages produce large amounts of proinflammatory cytokines, which are involved in resistance to pathogens, whereas M2 macrophages produce the anti-inflammatory mediators

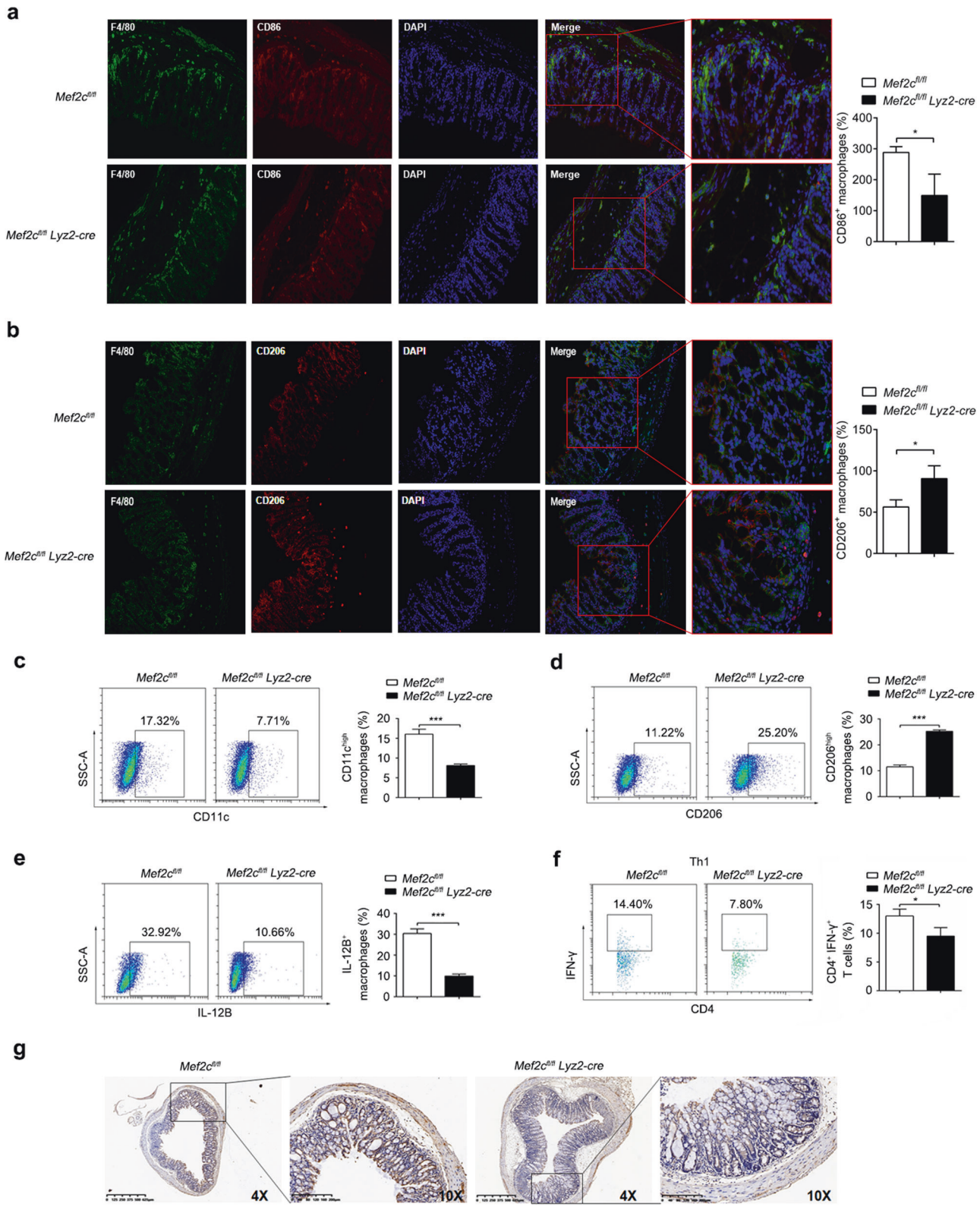

Fig. 7 *Mef2c* deficiency decreases proinflammatory macrophages and Th1 responses in experimental colitis. *Mef2c*$^{flox/flox}$ and *Mef2c*$^{flox/flox}$ *Lyz2-cre* mice were administered drinking water with or without 3% DSS for 7 days to induce acute colitis, followed by a 2-day recovery period with normal drinking water. **a** Immunofluorescence analysis of F4/80 and CD86 expression in the colon tissue of DSS-induced experimental colitis mice. **b** Immunofluorescence analysis of F4/80 and CD206 expression in the colon tissue of DSS-induced experimental colitis mice. Flow cytometric analysis of CD11c (**c**), CD206 (**d**) and (**e**) IL12B expression in macrophages from the colon tissue of DSS-induced experimental colitis mice. **f** Flow cytometric analysis of IFN-γ expression in CD4 T cells from the colon tissue of DSS-induced experimental colitis mice. **g** Immunohistochemical analysis of IFN-γ expression in the colon tissue of DSS-induced experimental colitis mice. The data are representative of three independent experiments. The data represent the mean ± SD. *$P < 0.05$, ***$P < 0.001$

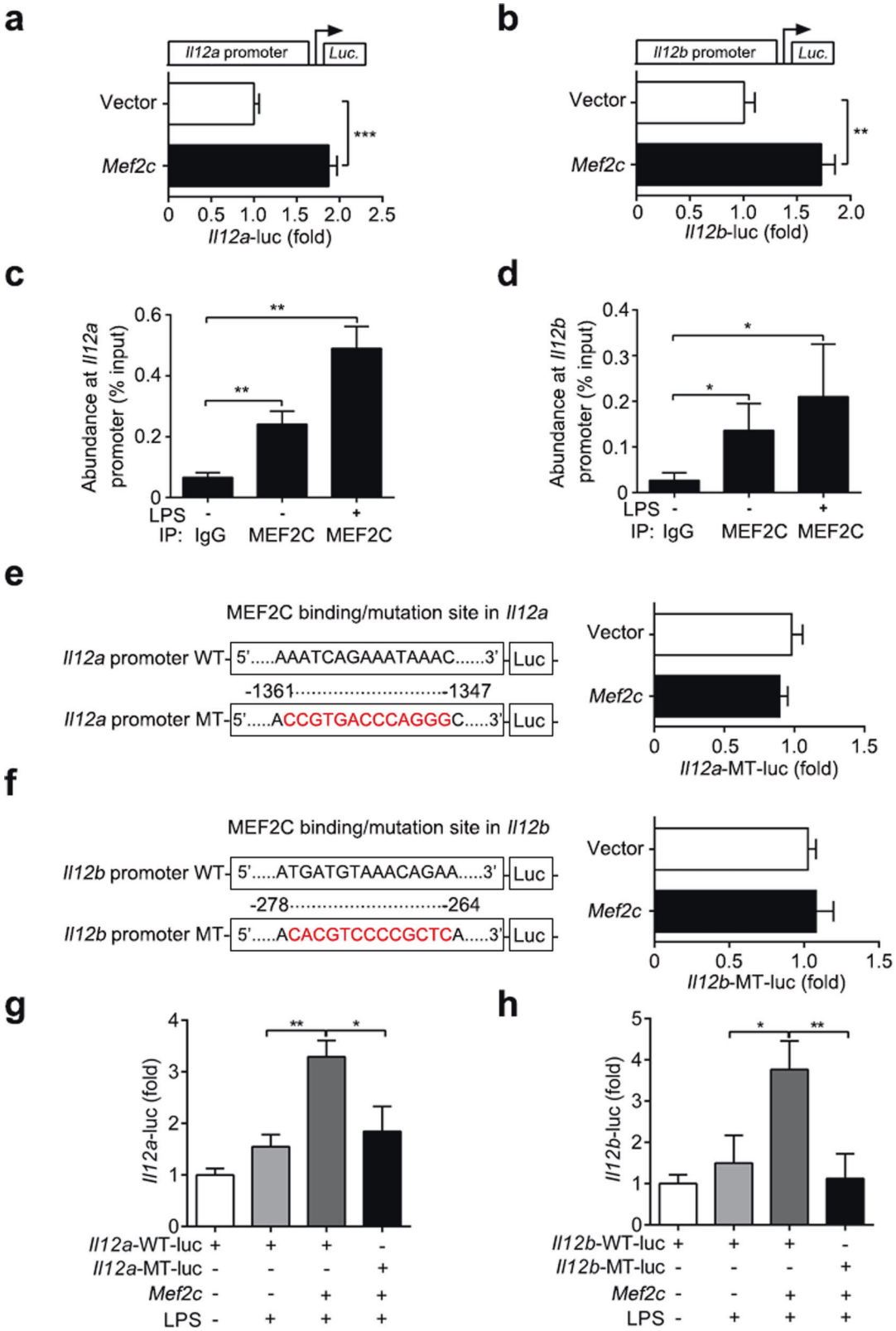

Fig. 8 MEF2C directly regulates the transcription of Il12*a* and Il12*b*. Dual-luciferase reporter assays were performed 24 h after the cotransfection of HEK 293 T cells with *Mef2c* plasmids and *Il12a* (**a**) and *Il12b* (**b**) luciferase reporter plasmids. ChIP assays were used to analyze MEF2C recruitment to the *Il12a* (**c**) and *Il12b* (**d**) promoters in peritoneal macrophages stimulated with or without LPS. Schematic diagrams of *Il12a* (**e**) and *Il12b* (**f**) mutant luciferase reporter plasmids (left). Dual-luciferase reporter assays were performed 24 h after the cotransfection of HEK 293 T cells with *Mef2c* plasmids and *Il12a* (**e**) and *Il12b* (**f**) mutant luciferase reporter plasmids. Raw 264.7 cells were transfected with *Mef2c* plasmids or wild-type and mutant *Il12a* (**g**) and *Il12b* (**h**) luciferase reporter plasmids for 24 h and then stimulated with LPS (100 ng/ml). Dual-luciferase reporter assays were performed. The data are representative of three independent experiments and represent the mean ± SD. $^{*}P < 0.05$, $^{**}P < 0.01$, $^{***}P < 0.001$

responsible for tissue repair and tumor progression [46]. qPCR analyses showed that *Mef2c* knockdown or knockout in macrophages inhibited LPS-induced expression of M1 macrophage markers (such as *Il12a*, *Il12b*, and *Il23a*), while the expression of M2 macrophage markers (such as *Il10*, *Arg1* and *Chil3*) was increased. Similarly, flow cytometric analysis demonstrated that CD11c (M1 macrophage marker) expression was downregulated in *Mef2c*-deficient macrophages, while CD206 (M2 macrophage marker) expression was upregulated, indicating that *Mef2c* influences M1 macrophage polarization. However, we did not find significant changes in the expression of *Il1b*, *Il6*, or *Tnf* in *Mef2c*-knockdown or -knockout macrophages compared to wild-type macrophages in vitro. These proinflammatory cytokines are commonly regarded as markers of M1 macrophages [6]. Although *Mef2c* has been reported to suppress NF-κB activation [47], our findings showed that *Mef2c* had no obvious effect on the NF-κB signaling pathway. It is possible that *Mef2c* has distinct functions in different cells and regulates macrophage polarization through an NF-κB-independent pathway. However, $Mef2c^{flox/flox}$ *Lyz2-cre* mice produced less IL-1β, IL-6 and TNF-α in response to *Listeria monocytogenes* compared to their wild-type counterparts, as determined by ELISA. Moreover, using a DSS-induced experimental colitis model, we showed that IL-1β, IL-6 and TNF-α production in the colons of $Mef2c^{flox/flox}$ *Lyz2-cre* mice was significantly decreased after colitis induction. These results suggest that although *Mef2c* does not directly affect the production of some proinflammatory cytokines, it influences macrophage phenotypes and functions, thus changing the microenvironment of the tissue in vivo and regulating the production of related cytokines.

In addition, M1 and M2 macrophages show distinctive glucose and amino acid metabolism. M1 macrophages exhibit a shift toward the glycolytic pathway, whereas oxidative phosphorylation is the dominant pathway in M2 macrophages [48, 49]. It can be suggested that this shift in macrophage metabolism improves the ability if cells to regulate responses to pathogen infection and inflammation. In addition, nitric oxide (NO), an inflammatory signaling molecule, plays an important role in inflammatory and antibacterial responses. In M1 macrophages, iNOS catalyzes the conversion of L-arginine to reactive nitrogen intermediates (RNIs), which have strong antimicrobial activity. In contrast, M2 macrophages have increased expression of ARG1, which catalyzes the conversion of L-arginine into ornithine and polyamines [50, 51]. Immunoblot analysis showed that iNOS expression was decreased in *Mef2c*-deficient macrophages, whereas ARG1 expression was increased. These findings suggest that *Mef2c* influences M1 macrophage polarization, and further studies of the mechanism are required to fully elucidate the biology of *Mef2c*.

Previous studies have shown that M1 macrophages facilitate inflammatory responses and resist pathogen infection [6]. Based on the ability of *Mef2c* to promote M1 macrophage polarization, we investigated the effects of LPS challenge or *Listeria monocytogenes* infection on $Mef2c^{flox/flox}$ *Lyz2-cre* mice. We found that *Mef2c* deficiency was associated with reduced production of proinflammatory cytokines under these conditions compared to those in wild-type mice. We also found that mice with myeloid-specific *Mef2c* knockout were more susceptible to *Listeria monocytogenes* infection than wild-type mice based on the higher bacterial loads in the spleen and liver and lower survival rates after *Listeria monocytogenes* infection.

ROS are essential for pathogen clearance [52] and play an important role in promoting the polarization of macrophages to a proinflammatory phenotype [53]. Our data showed that macrophages from $Mef2c^{flox/flox}$ *Lyz2-cre* mice produced less ROS and exhibited a reduced capacity to kill bacteria than those from wild-type mice, which is consistent with our observation that *Mef2c*-deficient mice had increased susceptibility to *Listeria monocytogenes* infection. Furthermore, the impaired Th1 response in $Mef2c^{flox/flox}$ *Lyz2-cre* mice after *Listeria monocytogenes* infection also accounts for the increased susceptibility of these mice to infection. While appropriate inflammatory responses can facilitate the clearance of pathogens, an excessive response leads to uncontrolled inflammation and the exacerbation of disease [54]. Using the DSS-induced experimental colitis model, we showed that the inflammatory response was impaired in $Mef2c^{flox/flox}$ *Lyz2-cre* mice, which had less severe colonic tissue damage than wild-type mice, and that these changes were associated with a decrease in M1 macrophages and a reduced Th1 response in the colon. Consequently, we conclude that *Mef2c* deficiency in macrophages results in impaired polarization toward the M1 phenotype.

To further clarify the mechanism by which *Mef2c* functions as a transcription factor to regulate macrophage polarization, we used the JASPAR database (http://jaspar.genereg.net/) to predict MEF2C binding sites in the promoter sequences of genes encoding macrophage lineage-specific cytokines. This analysis predicted the presence of an A/T-rich DNA consensus sequence in the promoters of the genes encoding *Il12a* and *Il12b*. Chromatin immunoprecipitation (ChIP) and double luciferase reporter assays showed that MEF2C bound to the promoters of the genes encoding the *Il12a* and *Il12b* subunits to increase their transcription. Previous studies have shown that macrophage polarization is regulated by many transcription factors, such as IRF5 and KLF4 [11, 55]. IRF5 directly activates *Il12a*, *Il12b* and *Il23a* transcription but represses *Il10* transcription. MEF2C also directly activates *Il12a* and *Il12b* transcription. Furthermore, our global gene expression analysis revealed a slight upregulation in KLF4 expression (approximately 1.35-fold), which could promote M2 macrophage polarization by interacting with STAT6. Therefore, it can be hypothesized that *Mef2c* coordinates with these transcription factors to influence the expression of macrophage lineage-specific genes.

In summary, our study demonstrated that *Mef2c* directly activated the transcription of *Il12a* and *Il12b* and then promoted M1 macrophage polarization and Th1 responses, resulting in resistance to *Listeria monocytogenes* infection and susceptibility to DSS-induced experimental colitis. In addition, we showed that *Mef2c* regulated the ability of macrophages to kill bacteria and produce ROS, but the detailed mechanism still needs further investigation. These findings provide new insights into the mechanism of macrophage polarization and reveals that *Mef2c* is a potential therapeutic target for inflammatory and autoimmune diseases.

REFERENCES

1. DeNardo DG, Ruffell B. Macrophages as regulators of tumour immunity and immunotherapy. Nat Rev Immunol. 2019;19:369–82.
2. Watanabe S, Alexander M, Misharin AV, Budinger GRS. The role of macrophages in the resolution of inflammation. J Clin Investig. 2019;129:2619–28.
3. Geissmann F, Manz MG, Jung S, Sieweke MH, Merad M, Ley K. Development of monocytes, macrophages, and dendritic cells. Science. 2010;327:656–61.
4. Diskin C, Ryan TAJ, O'Neill LAJ. Modification of proteins by metabolites in immunity. Immunity. 2021;54:19–31.
5. Phan AT, Goldrath AW, Glass CK. Metabolic and epigenetic coordination of T cell and macrophage immunity. Immunity. 2017;46:714–29.
6. Shapouri-Moghaddam A, Mohammadian S, Vazini H, Taghadosi M, Esmaeili SA, Mardani F, et al. Macrophage plasticity, polarization, and function in health and disease. J Cell Physiol. 2018;233:6425–40.
7. Ginhoux F, Guilliams M. Tissue-resident macrophage ontogeny and homeostasis. Immunity. 2016;44:439–49.
8. Murray PJ, Allen JE, Biswas SK, Fisher EA, Gilroy DW, Goerdt S, et al. Macrophage activation and polarization: nomenclature and experimental guidelines. Immunity. 2014;41:14–20.
9. Murray PJ. Macrophage polarization. Annu Rev Physiol. 2017;79:541–66.
10. Mosser DM, Hamidzadeh K, Goncalves R. Macrophages and the maintenance of homeostasis. Cell Mol Immunol. 2021;18:579–87.
11. Krausgruber T, Blazek K, Smallie T, Alzabin S, Lockstone H, Sahgal N, et al. IRF5 promotes inflammatory macrophage polarization and TH1-TH17 responses. Nat Immunol. 2011;12:231–8.
12. Ivashkiv LB. IFNgamma: signalling, epigenetics and roles in immunity, metabolism, disease and cancer immunotherapy. Nat Rev Immunol. 2018;18:545–58.

13. Fleetwood AJ, Lawrence T, Hamilton JA, Cook AD. Granulocyte-macrophage colony-stimulating factor (CSF) and macrophage CSF-dependent macrophage phenotypes display differences in cytokine profiles and transcription factor activities: implications for CSF blockade in inflammation. J Immunol. 2007;178:5245–52.
14. Pham THM, Brewer SM, Thurston T, Massis LM, Honeycutt J, Lugo K, et al. Salmonella-driven polarization of granuloma macrophages antagonizes tnf-mediated pathogen restriction during persistent infection. Cell host microbe. 2020;27:54–67.
15. Satoh T, Takeuchi O, Vandenbon A, Yasuda K, Tanaka Y, Kumagai Y, et al. The Jmjd3-Irf4 axis regulates M2 macrophage polarization and host responses against helminth infection. Nat Immunol. 2010;11:936–89.
16. Zhang YG, Li XZ, Luo ZG, Ma LY, Zhu SL, Wang ZS, et al. ECM1 is an essential factor for the determination of M1 macrophage polarization in IBD in response to LPS stimulation. Proc Natl Acad Sci USA. 2020;117:3083–92.
17. Mantovani A, Marchesi F, Malesci A, Laghi L, Allavena P. Tumour-associated macrophages as treatment targets in oncology. Nat Rev Clin Oncol. 2017;14: 399–416.
18. Colegio OR, Chu NQ, Szabo AL, Chu T, Rhebergen AM, Jairam V, et al. Functional polarization of tumour-associated macrophages by tumour-derived lactic acid. Nature. 2014;513:559–63.
19. Odegaard JI, Ricardo-Gonzalez RR, Goforth MH, Morel CR, Subramanian V, Mukundan L, et al. Macrophage-specific PPAR gamma controls alternative activation and improves insulin resistance. Nature. 2007;447:1116–20.
20. Im JH, Buzzelli JN, Jones K, Franchini F, Gordon-Weeks A, Markelc B, et al. FGF2 alters macrophage polarization, tumour immunity and growth and can be targeted during radiotherapy. Nat Commun. 2020;11:4064.
21. Trinchieri G. Interleukin-12 and the regulation of innate resistance and adaptive immunity. Nat Rev Immunol. 2003;3:133–46.
22. Teng MWL, Bowman EP, McElwee JJ, Smyth MJ, Casanova JL, Cooper AM, et al. IL-12 and IL-23 cytokines: from discovery to targeted therapies for immune-mediated inflammatory diseases. Nat Med. 2015;21:719–29.
23. Wojno EDT, Hunter CA, Stumhofer JS. The Immunobiology of the Interleukin-12 Family: Room for Discovery. Immunity. 2019;50:851–70.
24. Martinez FO, Sica A, Mantovani A, Locati M. Macrophage activation and polarization. Front Biosci-Landmrk. 2008;13:453–61.
25. Bastos KRB, Alvarez JM, Marinho CRF, Rizzo LV, Lima MRD. Macrophages from IL-12p40-deficient mice have a bias toward the M2 activation profile. J Leukoc Biol. 2002;71:271–8.
26. Murphy CA, Langrish CL, Chen Y, Blumenschein W, McClanahan T, Kastelein RA, et al. Divergent pro- and Antiinflammatory roles for IL-23 and IL-12 in joint autoimmune inflammation. J Exp Med. 2003;198:1951–7.
27. Yen D, et al. IL-23 is essential for T cell-mediated colitis and promotes inflammation via IL-17 and IL-6. J Clin Investig. 2006;116:1310–6.
28. Cante-Barrett K, Pieters R, Meijerink JPP. Myocyte enhancer factor 2C in hematopoiesis and leukemia. Oncogene. 2014;33:403–10.
29. Dietrich JB. The MEF2 family and the brain: from molecules to memory. Cell Tissue Res. 2013;352:179–90.
30. Clark RI, Tan SW, Péan CB, Roostalu U, Vivancos V, Bronda K, et al. MEF2 is an in vivo immune-metabolic switch. Cell. 2013;155:435–47.
31. Cilenti F, Barbiera G, Caronni N, Iodice D, Montaldo E, Barresi S, et al. A PGE(2)-MEF2A axis enables context-dependent control of inflammatory gene expression. Immunity. 2021;54:1665–82.
32. Wang IF, Wang YH, Yang YH, Huang GJ, Tsai KJ, Shen CKJ. Activation of a hippocampal CREB-pCREB-miRNA-MEF2 axis modulates individual variation of spatial learning and memory capability. Cell Rep. 2021;36:109477.
33. Sekiyama Y, Suzuki H, Tsukahara T. Functional Gene Expression Analysis of Tissue-Specific Isoforms of Mef2c. Cell Mol Neurobiol. 2012;32:129–39.
34. Potthoff MJ, Olson EN. MEF2: a central regulator of diverse developmental programs. Development. 2007;134:4131–40.
35. Fujii T, Murata K, Mun SH, Bae S, Lee YJ, Pannellini T, et al. MEF2C regulates osteoclastogenesis and pathologic bone resorption via c-FOS. Bone Res. 2021;9:4.
36. Tarumoto Y, Lin S, Wang JH, Milazzo JP, Xu YL, Lu B, et al. Salt-inducible kinase inhibition suppresses acute myeloid leukemia progression in vivo. Blood. 2020;135:56–70.
37. Tarumoto Y, Lu B, Somerville TDD, Huang YH, Milazzo JP, Wu XS, et al. LKB1, salt-inducible kinases, and MEF2C are linked dependencies in acute myeloid leukemia. Mol Cell. 2018;69:1017–27.
38. Deczkowska A, Matcovitch-Natan O, Tsitsou-Kampeli A, Ben-Hamo S, Dvir-Szternfeld R, Spinrad A, et al. Mef2C restrains microglial inflammatory response and is lost in brain ageing in an IFN-I-dependent manner. Nat Commun. 2017;8:717.
39. Wilker PR, Kohyama M, Sandau MM, Albring JC, Nakagawa O, Schwarz JJ, et al. Transcription factor Mef2c is required for B cell proliferation and survival after antigen receptor stimulation. Nat Immunol. 2008;9:603–12.
40. Bouttier M, Laperriere D, Memari B, Mangiapane J, Fiore A, Mitchell E, et al. Alu repeats as transcriptional regulatory platforms in macrophage responses to M-tuberculosis infection. Nucleic Acids Res. 2016;44:10571–87.
41. Ruffell B, Chang-Strachan D, Chan V, Rosenbusch A, Ho CM, Pryer N, et al. Macrophage IL-10 Blocks CD8(+) T cell-dependent responses to chemotherapy by suppressing IL-12 expression in intratumoral dendritic cells. Cancer Cell. 2014;26:623–37.
42. Cappiello MG, Sutterwala FS, Trinchieri G, Mosser DM, Ma XJ. Suppression of IL-12 transcription in macrophages following Fc gamma receptor ligation. J Immunol. 2001;166:4498–506.
43. Wang IM, Contursi C, Masumi A, Ma XJ, Trinchieri G, Ozato K. An IFN-gamma-inducible transcription factor, IFN consensus sequence binding protein (ICSBP), stimulates IL-12 p40 expression in macrophages. J Immunol. 2000;165:271–9.
44. Sanjabi S, Hoffmann A, Liou HC, Baltimore D, Smale ST. Selective requirement for c-Rel during IL-12 P40 gene induction in macrophages. Proc Natl Acad Sci USA. 2000;97:12705–10.
45. Mosser DM, Edwards JP. Exploring the full spectrum of macrophage activation. Nat Rev Immunol. 2008;8:958–69.
46. Mantovani A, Sica A, Locati M. Macrophage polarization comes of age. Immunity. 2005;23:344–6.
47. Xu Z, Yoshida T, Wu L, Maiti D, Cebotaru L, Duh EJ. Transcription factor MEF2C suppresses endothelial cell inflammation via regulation of NF-kappaB and KLF2. J Cell Physiol. 2015;230:1310–20.
48. Rodriguez-Prados JC, Través PG, Cuenca J, Rico D, Aragonés J, Martín-Sanz P, et al. Substrate fate in activated macrophages: a comparison between innate, classic, and alternative activation. J Immunol. 2010;185:605–14.
49. Vats D, et al. Oxidative metabolism and PGC-1 beta attenuate macrophage-mediated inflammation. Cell Metab. 2006;4:13–24.
50. Lemos H, Huang L, Prendergast GC, Mellor AL. Immune control by amino acid catabolism during tumorigenesis and therapy. Nat Rev Cancer. 2019;19:162–75.
51. Grohmann U, Bronte V. Control of immune response by amino acid metabolism. Immunological Rev. 2010;236:243–64.
52. West AP, Brodsky IE, Rahner C, Woo DK, Erdjument-Bromage H, Tempst P, et al. TLR signalling augments macrophage bactericidal activity through mitochondrial ROS. Nature. 2011;472:476–543.
53. Yuan Y, Chen Y, Peng T, Li L, Zhu W, Liu F, et al. Mitochondrial ROS-induced lysosomal dysfunction impairs autophagic flux and contributes to M1 macrophage polarization in a diabetic condition. Clin Sci. 2019;133:1759–77.
54. Liu YC, Zou XB, Chai YF, Yao YM. Macrophage polarization in inflammatory diseases. Int J Biol Sci. 2014;10:520–9.
55. Liao X, Sharma N, Kapadia F, Zhou G, Lu Y, Hong H, et al. Kruppel-like factor 4 regulates macrophage polarization. J Clin Investig. 2011;121:2736–49.

ACKNOWLEDGEMENTS

This work was supported by grants from the National Key Research and Development Program of China (2016YFA0502201) awarded to Prof. Huazhang An; the National Natural Science Foundation of China (Nos. U1801283, 31870908), the Guangdong Provincial Science and Technology Program (No. 2019B030301009) and the SZU Top Ranking Project (No. 86000000210) awarded to Prof. Weilin Chen; the National Natural Science Foundation of China (No. 81771711) awarded to Prof. Wengang Song; and the Guangdong Provincial Science and Technology Program (No. 2019A1515110086) awarded to Xibao Zhao. We thank Jessica Kate Tamanini (Scientific Editor, Shenzhen University School of Medicine) for editing the manuscript.

AUTHOR CONTRIBUTIONS

XZ, HA, and WC participated in the research design. XZ, QD, HL, and JQ conducted the experiments. JL, ZZ, WS, QD, YX, HW, and ZW contributed analytic tools or new reagents. XZ, WC, and HA performed the data analysis. XZ, WC, and HA contributed to the writing of the manuscript.

COMPETING INTERESTS

The authors declare no competing interests.

ADDITIONAL INFORMATION

Supplementary information The online version contains supplementary material available at https://doi.org/10.1038/s41423-022-00841-w.

Correspondence and requests for materials should be addressed to Huazhang An or Weilin Chen.

Reprints and permission information is available at http://www.nature.com/reprints